Research Square

Preprints are preliminary reports that have not undergone peer review.
They should not be considered conclusive, used to inform clinical practice,
or referenced by the media as validated information.

Expanding the flavonoid production in Acinetobacter baylyi ADP1 from lignin-derived aromatics

Kesi Kurnia
Tampere University
Aarni Mäkelä
Tampere University
Elena Efimova
Tampere University
Vasyl V. Mykuliak
Tampere University
Vesa P. Hytönen
Tampere University
Ville Santala
Tampere University
Suvi Santala
suvi.santala@tuni.fi
Tampere University

Research Article

Keywords:

Posted Date: September 10th, 2026

DOI: https://doi.org/10.21203/rs.3.rs-10892699/v1

License: This work is licensed under a Creative Commons Attribution 4.0 International License.
Read Full License

Additional Declarations: No competing interests reported.

Expanding the flavonoid production in *Acinetobacter baylyi* ADP1 from lignin-derived aromatics

Kesi Kurnia[1], Aarni Mäkelä[1], Elena Efimova[1], Vasyl V. Mykuliak[2], Vesa P. Hytönen[2,3], Ville Santala[1], Suvi Santala[1,*]

[1]Faculty of Engineering and Natural Sciences, Tampere University, Finland

[2]Faculty of Medicine and Health Technology, Tampere University, Finland

[3]Fimlab Laboratories, Tampere, Finland

[*]Correspondence: suvi.santala@tuni.fi

Abstract

Background

Flavonoids are valuable plant secondary metabolites with broad applications in the food, nutraceutical, cosmetic, and pharmaceutical industries. While microbial biosynthesis offers a renewable alternative for chemical synthesis and plant extraction, most production platforms rely on long synthesis pathways from sugars, requiring extensive pathway engineering and often focusing on individual products. Lignin-derived aromatics (LDAs) offer attractive precursors for flavonoid biosynthesis, but their utilization requires a host capable of aromatic substrate tolerance and metabolism.

Results

We engineered *Acinetobacter baylyi* ADP1 as a platform for the conversion of LDAs into multiple flavonoid products. We identified a novel heterologous enzyme combination CHS–CHI (CHS from *Stenoloma chusanum*-CHI from *Medicago sativa*) that supported efficient flavanone biosynthesis, namely 3.7 mg/L homoeriodictyol and 24.2 mg/L eriodictyol in flask cultivations. In fed-batch bioreactors, the engineered strain produced three flavonoids (homoeriodictyol, eriodictyol, and naringenin) from different aromatic substrates (ferulate, caffeate, *p*-coumarate), enabling product switching through feedstock selection without additional genetic engineering. Finally, flavonoid production was demonstrated directly from alkaline pretreated liquors (APLs) derived from wheat straw and organosolv lignin, demonstrating the relevance and compatibility of the platform with complex lignin-derived feedstocks.

Conclusions

This work establishes *A. baylyi* ADP1 as a versatile platform for the production of multiple flavonoids from LDAs. By leveraging native aromatic catabolism, the platform bypasses the need for extensive precursor biosynthesis and enables substrate-driven product diversification. The demonstrated compatibility with lignin-derived liquors highlights the potential of *A. baylyi* ADP1 as a platform for sustainable flavonoid production and lignin valorization in future applications.

Background

Flavonoids are a diverse family of plant-derived polyphenolic compounds. They play important roles in plant physiology, including protection against ultraviolet (UV) radiation, oxidative stress, and pathogen attack, while also contributing to pigmentation, signaling, and plant-microbe interactions [1,2]. Structurally, flavonoids share a common C6–C3–C6 carbon skeleton and comprise a wide range of subclasses, including flavanones, flavones, flavonols, chalcones, and anthocyanins [3]. Beyond their biological functions in plants, flavonoids have attracted considerable attention as high-value natural products because of their broad range of pharmacological activities and applications in the pharmaceutical, nutraceutical, cosmetic, and food industries [1,2]. Among these compounds, the flavanone naringenin (NAR) is particularly notable as both a bioactive molecule and a key intermediate for the biosynthesis of numerous downstream flavonoids [2,4]. NAR exhibits antioxidant, anti-inflammatory, antimicrobial, and antiviral activities, including reported in vitro activity against SARS-CoV-2 [5,6]. Structurally related flavanones, such as homoeriodictyol (HOM) and eriodictyol (ERI) are also of growing interest due to their distinct bioactivities and physicochemical properties. In particular, *O*-methylated derivatives such as HOM may offer advantages including improved metabolic stability, enhanced oral bioavailability, and altered biological activity relative to their unmethylated counterparts [7,8]. Despite their potential, flavonoid production remains largely dependent on plant extraction or chemical synthesis, both of which are constrained by low yields, complex purification, environmental burden, and limited scalability [9–11].

Microbial cell factories have emerged as a promising alternative for flavonoid production, offering advantages in sustainability, scalability, and process controllability. Through the heterologous expression of plant-derived biosynthetic enzymes, including chalcone synthase (CHS) and chalcone isomerase (CHI), engineered microorganisms can be programmed to

produce flavonoids with precise structural control and reproducible yields [12,13]. To date, most microbial flavonoid production platforms have been developed in a limited number of model hosts, particularly *Escherichia coli* [11,14,15] and *Saccharomyces cerevisiae* [9,16,17]. In these systems, flavonoid biosynthesis is typically established through *de novo* reconstruction of phenylpropanoid pathways that convert sugar-based carbon sources such as glucose into aromatic precursors, followed by activation to their corresponding CoA thioesters and subsequent condensation into flavonoid scaffolds [9,18]. While these approaches have enabled the production of flavonoids, they require the aromatic precursor structure to be synthesized *de novo* from central metabolites, often involving lengthy heterologous pathways and extensive metabolic rewiring that can increase metabolic burden and competition for cellular resources [19]. The challenge becomes even greater when expanding biosynthesis beyond common flavonoids such as NAR toward structurally diverse derivatives. Such pathway expansion frequently requires additional tailoring reactions, including hydroxylation and methylation, which rely on enzymes such as cytochrome P450 monooxygenases [20] and S-adenosylmethionine (SAM)-dependent methyltransferases [21]. Consequently, most microbial platforms have focused on the production of individual flavonoids through linear pathway optimization, whereas the efficient biosynthesis of multiple flavonoids within a single host remains underexplored. Therefore, developing strategies that simplify precursor supply while enabling access to diverse flavonoid structures remains an important challenge in microbial flavonoid engineering.

In this context, lignin has emerged as a strategically important yet still underutilized biomass fraction [22–24]. As a major structural polymer in plant cell walls, lignin is the second most abundant natural polymer on Earth after cellulose and represents one of the largest renewable reservoirs of aromatic carbon in nature [23,25,26]. Large quantities of lignin are generated

annually as low-value side streams from the pulp and paper industry and agricultural processing [27–29], yet the overwhelming majority is still combusted for heat and energy rather than upgraded into higher-value products [22]. Unlike cellulose and hemicellulose, which primarily yield sugars, lignin is composed of aromatic phenylpropanoid monomers: *p*-coumaryl alcohol, coniferyl alcohol, and sinapyl alcohol that give rise to the *p*-hydroxyphenyl (H), guaiacyl (G), and syringyl (S) units, respectively [23,30]. Consequently, lignin valorization into high-value chemicals and natural products is increasingly recognized as a key component of a circular bioeconomy, improving the economic viability and resource efficiency of lignocellulosic biorefineries [31].

Depolymerization of lignin generates a diverse mixture of aromatic compounds, including hydroxycinnamic acids such as *p*-coumarate and ferulate [32–35], which are structurally related to key intermediates in flavonoid biosynthesis [36]. In contrast to glucose-based *de novo* biosynthesis, these compounds provide preformed aromatic scaffolds that can be directly redirected toward flavonoid production, reducing the need to reconstruct the corresponding aromatic precursors from central metabolism. However, most established production hosts are poorly suited for direct flavonoid production from lignin-derived feedstocks. For example, *E. coli* and *S. cerevisiae* typically require additional heterologous pathway engineering, including expression of 4-coumarate-CoA ligase (4CL), to activate hydroxycinnamic acids into the corresponding CoA thioesters for flavonoid biosynthesis [8,9,37,38]. Even then, they lack the native aromatic catabolic pathways required to assimilate the diverse aromatic constituents present in lignin hydrolysates. As a result, a substantial fraction of the carbon present in lignin hydrolysates remains inaccessible. Furthermore, lignin hydrolysates often contain elevated concentrations of aromatic compounds and process-derived by-products [35,39], which can further impair growth and production performance. Together, these considerations highlight

the potential value of microbial hosts with native aromatic metabolic capabilities and tolerance toward lignin-derived compounds for exploiting lignin-derived feedstocks in flavonoid production.

Acinetobacter baylyi ADP1 (hereafter ADP1) represents an attractive microbial chassis for lignin valorization due to its native capacity to uptake and metabolize a broad range of aromatic compounds through the β-ketoadipate pathway [40–42]. Unlike conventional flavonoid-producing hosts such as *E. coli* and *S. cerevisiae*, ADP1 naturally metabolizes numerous lignin-derived compounds, including hydroxycinnamates and benzoates, enabling the direct utilization of aromatic feedstocks. Furthermore, ADP1 exhibits exceptional genetic tractability owing to its natural competence and highly efficient homologous recombination machinery, facilitating rapid genome engineering and pathway construction [43–45]. In addition to its well-characterized aromatic metabolism, ADP1 has been shown to tolerate high concentrations of LDA compounds [46,47] and to support the biosynthesis of value-added products from renewable feedstocks [13,34,48,49]. These characteristics make ADP1 particularly well suited for coupling LDA assimilation with heterologous biosynthetic pathways. Indeed, our previous work established ADP1 as a platform for NAR production from *p*-coumarate, demonstrating the feasibility of flavonoid biosynthesis in this host [13]. Together, these characteristics position ADP1 as a promising chassis for flavonoid diversification, enabling the sustainable conversion of diverse LDA compounds into multiple high-value flavonoid products.

In this study, we establish a lignin-to-flavonoid platform in ADP1 that enables production of multiple high-value flavonoids from diverse LDA compounds (ferulate, caffeate, and *p*-coumarate) (Fig 1). Through CHS screening and evaluation under different cultivation

conditions, we demonstrate that a single engineered chassis can produce distinct flavonoid products depending on the supplied aromatic precursor, as well as multiple products simultaneously from mixed aromatic substrates. This substrate-directed strategy enables flavonoid diversification without extensive pathway reconfiguration, providing a flexible route to access structurally diverse compounds from renewable feedstocks. Importantly, we extend this strategy from defined aromatic substrates to complex lignin-derived streams, demonstrating flavonoid production directly from alkaline pretreated liquor (APL) derived from wheat straw and straw-derived organosolv lignin. Collectively, this work expands the substrate and product scope of flavonoid biosynthesis in ADP1 and highlights its potential as a platform for converting LDAs into multiple flavonoid products.

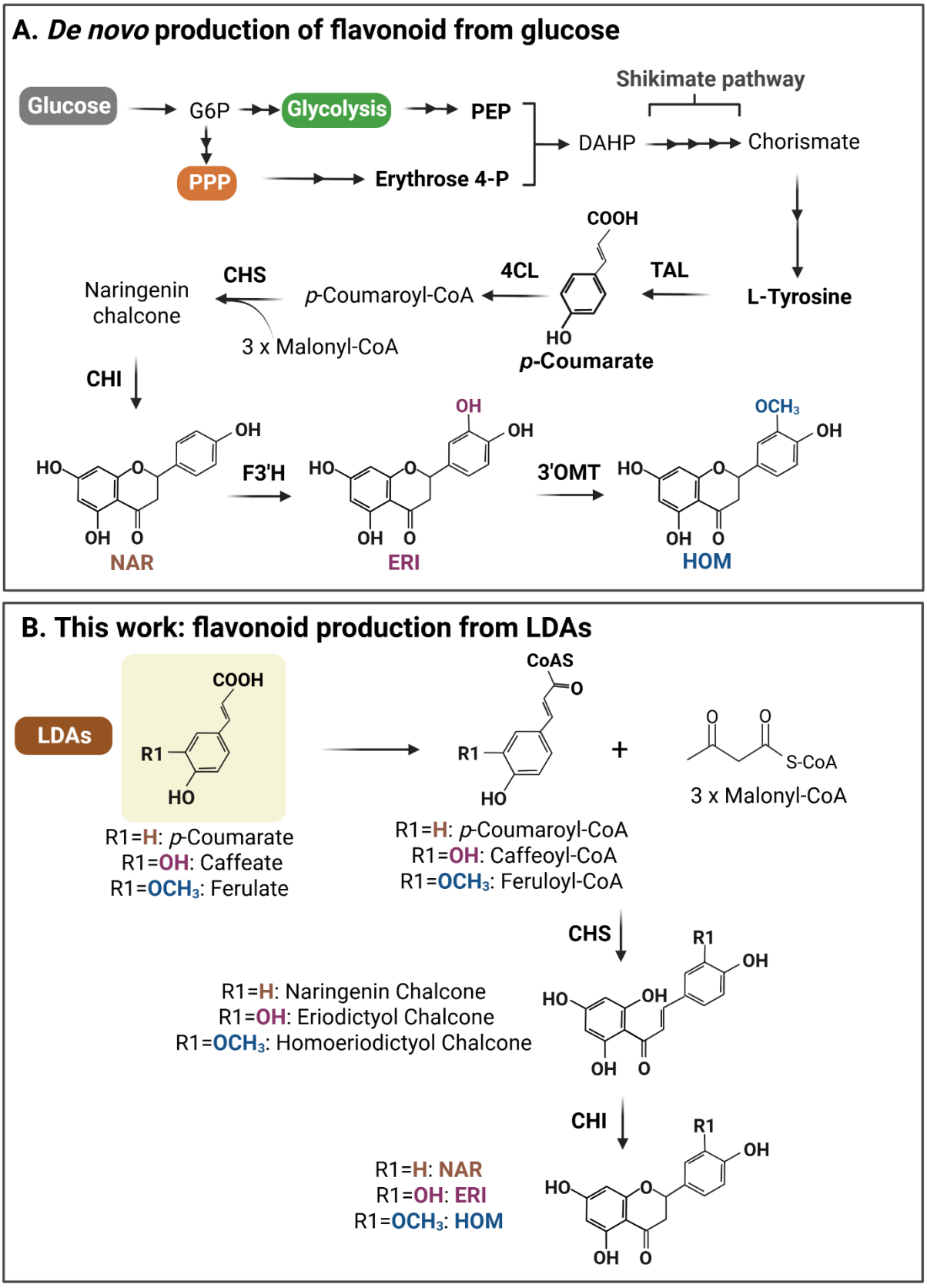


Figure 1. Comparison of flavonoid production from glucose and lignin-derived aromatics (LDAs). (A) *De novo* flavonoid production from glucose requires carbon flux through the

multistep shikimate pathway to generate the aromatic precursor *p*-coumarate, with additional pathway engineering required to access different flavonoid products. (B) In contrast, LDA-based production bypasses *de novo* aromatic precursor biosynthesis by using LDAs as direct precursors, with different aromatic substrates directing the production of distinct flavonoids (NAR, ERI, and HOM) and mixed substrates enabling their simultaneous production within a single engineered system. 4CL, 4-coumarate-CoA ligase; TAL, tyrosine ammonia-lyase; CHS, chalcone synthase; CHI, chalcone isomerase; F3′H, flavonoid 3′-hydroxylase; 3′OMT, flavonoid 3′-*O*-methyltransferase; NAR, naringenin; ERI, eriodictyol; HOM, homoeriodictyol.

Methods

Bacterial strains and culture conditions

The bacterial strains used in this study are described in Supplementary Table S1. *Escherichia coli* XL1-Blue (Stratagene, USA) was used for the plasmid constructions and amplifications. The constructed strain ASA803 derived from *A. baylyi* ADP1 (DSM 24193, DSMZ, Germany) was used as the parental strain for strain construction [13]. *E. coli* and ADP1 strains were incubated at 30 °C. Strains were maintained on low salt Lysogeny broth (LB) or mineral salts medium (MSM). For grown-on plates, 1.5% agar (w/v) was added. The MSM consists of: (per Liter; 3.88 g K_2HPO_4, 1.63 g NaH_2PO_4, 2.0 g $(NH_4)_2SO_4$, pH 7.0). The MSM was supplemented with a trace elements solution (per Liter; 10 mg/L ethylenediaminetetraacetic acid (EDTA), 0.1 g/L $MgCl_2.6H_2O$, 2 mg/L $ZnSO_47H_2O$, 1 mg/L $CaCl_2{\cdot}2H_2O$, 5 mg/L $FeSO_4{\cdot}7H_2O$, 0.2 mg/L, $Na_2MoO_4{\cdot}2H_2O$, 0.2 mg/L $CuSO_4{\cdot}5H_2O$, 0.4 mg/L $CoCl_2{\cdot}6H_2O$, 1 mg/L $MnCl_2{\cdot}2H_2O$). For liquid cultivation, pre-cultures were grown in MGC (MSM with 50 mM gluconate, 0.2% (w/v) casamino acids), and the appropriate antibiotics. Unless otherwise stated, main cultures were

prepared in the same medium supplemented with aromatic substrates and inducers as indicated in each experiment. The stock solution of, ferulate, caffeate, and *p*-coumarate were prepared with a concentration of 100 mM (pH 8.3-8.5). When required, antibiotics were added to the medium at the following final concentrations: ampicillin (Amp) 100 µg/mL, kanamycin (Km) 50 µg/mL, and chloramphenicol (Cm) 25 µg/mL. Cyclohexanone stock solution (100 mM) was prepared in water. Ferulate was purchased from Sigma-Aldrich (USA), caffeate and *p*-coumarate were purchased from TCI (Japan). HOM and ERI were purchased from Extrasynthese (France), whereas NAR analytical standard was purchased from Sigma Aldrich (USA).

Structural analysis and mutagenesis of CHS

Candidate residues for mutagenesis were identified through combined structural and sequence conservation analyses. The crystal structure of CHS *Stenoloma chusanum* (ScCHS1) (PDB id: 7YJB) and the AlphaFold-predicted structure of CHS *Hypericum androsaemum* (HaCHS) (UniProt id: Q9FUB7) were used as structural references. Multiple sequence alignment of CHS homologs was performed using Clustal Omega (EMBL-EBI web server; https://www.ebi.ac.uk/jdispatcher/msa/clustalo) [50], and residue conservation scores were calculated with the ConSurf web server [51]. Structural comparison between ScCHS1 and HaCHS, together with inspection of residues lining the substrate/product channel, was performed in PyMOL (Schrödinger, LLC). Based on these analyses, three residues were selected for site-directed mutagenesis, and the corresponding mutant constructs were generated by USER cloning [52]. The resulting plasmids were transformed into *E. coli* XL1-Blue by electroporation, screened by colony PCR, and confirmed by Sanger sequencing (Macrogen,

Netherlands). Sequence-verified plasmids were subsequently transformed into ADP1 by natural transformation and selected on LB agar containing chloramphenicol (Cm).

Plasmid and strain construction

The plasmids and primers used in this study are listed in Supplementary Tables S2 and S3, respectively. PCR amplifications were performed using Phusion™ Hot Start II High-Fidelity DNA Polymerase (Thermo Fisher Scientific, USA). Colony PCR was performed using OneTaq™ Quick-Load 2× Master Mix (New England Biolabs, USA).

Plasmids pHOM1 and pHOM2 were constructed as follows. Genes encoding chalcone synthase (*CHS*) variants previously reported to accept feruloyl-CoA, *ScCHS1* (PDB id: 7YJB) [53] and *HvCHS2* (PDB id: 8B3C) [8], were selected for this study. The genes were synthesized and codon-optimized for ADP1 (GenScript Biotech, Netherlands), with flanking restriction sites and a ribosome binding site (BBa_B0034). Each *CHS* gene was cloned into pBAV1C-chn [13,54] using the BioBrick assembly standard via XbaI/SpeI and PstI restriction sites. The resulting plasmids were then digested with XbaI and PstI, and *Medicago sativa* chalcone isomerase (*MsCHI*) (KF765782.1), previously shown to enhance NAR production [13], was inserted downstream of *CHS*. The assembled plasmids were first transformed into *E. coli* XL1-Blue for verification, and confirmed constructs were subsequently transformed into ADP1 as described above. Gene sequences are provided in Supplementary Table S4.

Shake flask cultivation

Glycerol stocks were streaked onto LB agar plates supplemented with 25 mM glucose and 25 µg/mL chloramphenicol (Cm). Single colonies were used to inoculate precultures in the defined

medium described above and incubated overnight at 30 °C with agitation at 300 rpm. Precultures were harvested by centrifugation at 6000 × g for 6 min, the supernatant was discarded, and the cell pellets were resuspended in mineral salts medium (MSM) lacking a carbon source to concentrate biomass. The resuspended cells were used to inoculate 100-mL baffled Erlenmeyer flasks containing 20 mL MGC medium, with composition identical to the preculture medium and supplemented with aromatics and inducers as indicated. Chloramphenicol was added from an aqueous stock solution (25 µg/mL) to avoid ethanol carryover as a carbon source. Cultures were inoculated at an initial OD_{600} of 0.8, unless otherwise specified. Aromatic substrates (ferulate and caffeate) were added at concentrations specified in each experiment, and heterologous pathway expression was induced with 0.5 µM cyclohexanone. All cultivations were performed in biological triplicates and incubated for 72 h.

Metabolite analysis

Optical density at 600 nm (OD_{600}) was measured using UV-Vis spectrophotometer (UV-1990i, Shimadzu, Japan). For flavanone quantification (HOM, NAR, and ERI), culture broth was extracted with an equal volume of ethyl acetate, vortexed for 30 s, and incubated on a rotary mixer at room temperature for 2 h as previously described [13,53,55]. After centrifugation for 5 min, the organic phase was collected and evaporated overnight. The dried residue was resuspended in methanol and subjected to HPLC analysis. For quantification of aromatic compounds (ferulate, caffeate, and *p*-coumarate), culture samples were centrifuged at 20,000 × *g* for 5 min. The clarified supernatants were filtered through syringe filters (CHROMAFIL® PET, PET-45/25, Macherey–Nagel, Germany) and analyzed by HPLC. Identification of

flavanones and aromatic substrates were performed using liquid chromatography coupled to photodiode-array detection (Shimadzu Nexera LC-40, Japan). Luna C18(2) (100Å 4.6 x 150 mm, 5 µ) was used as the column and placed at 40 °C.

For experiments requiring separation of a single flavonoid and its corresponding aromatic precursor, an isocratic method was used as previously described [13]. The mobile phase consisted of 60% (0.1% formic acid) and 40% (MeOH) a flow rate 1 mL/min. For experiments involving simultaneous analysis of multiple flavonoids and aromatic compounds, a gradient method was applied. The mobile phases consisted of eluent A (water:methanol:formic acid, 80:20:0.16, v/v/v) and eluent B (100% methanol). Separation was performed using the following gradient program: 100% eluent A for 20 min, to 75% eluent at 22 min, 75% eluent A from 22 to 40 min, to 100% eluent A at 42 min, 100% eluent A from 42 to 47 min. The flow rate was set to 1 mL/min, and the injection volume was 5 µL. Flavanones were detected at 288 nm, with retention time of approximately 29.88 min (ERI), 36.97 min (NAR), and 37.9 min (HOM). Aromatic substrates were detected at their respective wavelengths: ferulate at 318 nm, caffeate at 318 nm, and *p*-coumarate at 304 nm. Compound concentrations were determined using calibration curves prepared from the corresponding chemical standards.

LC-MS analysis

LC-MS analysis was done on Agilent 1260 Infinity chromatograph connected with AccuTOF LCplus (JMC-T100LP, Japan) high resolution mass spectrometer with an electrospray ionization source (ESI). Agilent InfinityLab Poroshell EC-18 column (4.6 x 100 mm, 2 µ) was maintained at 30˚C. 2 µL of analytes were injected. Isocratic elution was performed at a flow rate of 0.2

mL/min with a mixture of 0.1% formic acid/methanol 1/1 as the mobile phase. Detection was performed in negative mode (ESI^-).

Fed-batch bioreactor cultivation

Fed-batch cultivations were performed in a 250-mL mini bioreactor (Applikon Biotechnology, The Netherlands) with an initial working volume of 50 mL. Cultivation conditions and process control parameters were applied as previously described [13]. The feed solution, consisting of 50 mM gluconate, 0.2% casamino acids, and 1.3 mM each of ferulate, caffeate, and *p*-coumarate in MSM, was supplied at a rate of 3.7 mL/h for 48 h. When necessary, foaming was controlled by the addition of small volumes of a 10% (v/v) Antifoam A (Sigma-Aldrich, USA). Samples (2 mL) were collected aseptically throughout the cultivation for analysis of cell growth, aromatic substrates, and flavanones. Bioreactor experiments were performed in duplicate.

Preparation of alkaline pretreated liquor (APL)

APLs were prepared from wheat straw and straw-derived organosolv lignin (a kind gift from Fortum, Finland). Wheat straw was subjected to alkaline pretreatment at 130 °C using 70 mg NaOH per g dry biomass [39], whereas straw-derived organosolv lignin was treated at 130 °C with 2% NaOH (w/w dry biomass) [56]. Prior to use, the resulting liquor was processed by centrifugation at 10,000 x g, 10 °C for 30 min to remove the bulk solids. The pH was then adjusted to 7.0 using 5 M H_2SO_4, followed by a second centrifugation step at 10,000 x g, 10 °C for 30 min. The resulting supernatant was subsequently filter-sterilized through 0.20-0.45 µm filter, followed by HPLC analysis to quantify the aromatic compounds. Filter-sterilized APL was

added to cultures at final concentration corresponding to 0.5 mM *p*-coumarate equivalents, in the presence of 50 mM gluconate and 0.2% casamino acids as supplementary carbon sources.

Results

HOM production from ferulate in ADP1

Biosynthesis of HOM involves two reactions catalyzed by CHS and CHI. CHS catalyzes the condensation of one molecule of feruloyl-CoA with three molecules of malonyl-CoA to form homoeriodictyol chalcone, which is subsequently cyclized by CHI to yield HOM. In our previous study, ASA806 strain was established as platform for NAR production from *p*-coumarate [13]. The strain harbors heterologous CHS from *Hypericum androsaemum* (*HaCHS*) and CHI from *M. sativa* (*MsCHI*), together with deletion of the *hcaA* gene to block native *p*-coumarate catabolism. Engineering strategies aimed at increasing malonyl-CoA availability were also evaluated previously but did not improve NAR production [13]. Therefore, rather than further modifying precursor supply, the present study focused on expanding the substrate and product scope of the established ASA806 platform.

As HOM biosynthesis relies on the same CHS–CHI module, we next investigated whether the existing ASA806 platform could be extended toward HOM production from ferulate. To this end, we pursued two complementary strategies: engineering CHS substrate specificity and screening heterologous CHS orthologs compatible with feruloyl-CoA utilization. Unlike *p*-coumarate, ferulate contains a methoxy substitution that enables the biosynthesis of HOM through a distinct feruloyl-CoA-derived chalcone intermediate. However, previous study has shown that *HaCHS* exhibits poor utilization of feruloyl-CoA [57], thereby limiting HOM biosynthesis. Intrigued by this limitation, we investigated whether mutagenesis of CHS could

improve accommodation of the *O*-methylated substrate. We therefore pursued a structure-guided engineering strategy to expand CHS substrate specificity toward feruloyl-CoA. To guide mutagenesis, an AlphaFold-predicted model of *Ha*CHS (UniProt id: Q9FUB7) was used and compared with the crystal structure of *Sc*CHS1 (PDB id: 7YJB) to identify candidate residues associated with starter-CoA recognition (Supplementary Fig. S1-S2). Two residues located proximal to the substrate-binding pocket were selected for mutagenesis based on sequence differences from a feruloyl-CoA-accepting CHS homologue. Substitution of these residues was hypothesized to increase the available space within the substrate-binding pocket and facilitate accommodation of the *O*-methyl group of feruloyl-CoA. A third residue was targeted to alter the electrostatic environment of the active site. As no high-throughput biosensor or screening assay was available for HOM production, the analysis was restricted to three rationally selected *CHS* variants: E192Q, V196I, F165Y. The resulting strains harboring CHS^{E192Q}, CHS^{V196I}, and CHS^{F165Y} were designated ASA812, ASA813, and ASA814, respectively.

However, similar to the wild-type enzyme, none of the engineered CHS variants produced detectable levels of HOM under the tested conditions (Supplementary Fig. S3). To determine whether the introduced mutations impaired overall CHS activity, the variants were additionally evaluated using *p*-coumarate as a substrate. Most mutants retained catalytic functionality and supported NAR production, with the exception of ASA812 (Supplementary Fig. S4), indicating that the lack of HOM production was not simply due to loss of CHS function. In separate experiments, the strains also did not grow on ferulate while externally supplied HOM did not exhibit detectable toxicity toward the host strain (Supplementary Fig. S5-S6), suggesting that the absence of HOM production was unlikely to result from precursor loss through native metabolism or product inhibition. Together, these results suggest that point mutagenesis of

the parental CHS scaffold was insufficient to enable efficient feruloyl-CoA utilization within the tested chassis and cultivation conditions. We therefore next shifted our strategy toward screening heterologous CHS orthologs previously reported to accept feruloyl-CoA-derived substrates.

Although CHSs are widely distributed, most characterized enzymes preferentially utilize *p*-coumaroyl-CoA, and activity toward feruloyl-CoA has been demonstrated for only a limited number of homologues. We therefore used a focused screening strategy, selecting *CHS* orthologs from *ScCHS1* [53] and *HvCHS2* [8], both previously associated with feruloyl-CoA utilization and HOM biosynthesis. The corresponding genes were codon-optimized for expression in ADP1 and paired with the *MsCHI*, which has previously been shown to improve flavonoid production in this host [13], generating constructs pHOM1 and pHOM2 (Fig. 2A). The plasmids were subsequently introduced into ADP1 by natural transformation, generating the strains ASA815 and ASA816, respectively. Under ferulate-supplemented conditions, both heterologous *CHS* modules enabled production of HOM (Fig. 2B). Final titers reached 1.8 mg/L and 1.0 mg/L after 24 h for ASA815 and ASA816, respectively. In addition, LC–MS analysis confirmed the identity of the product as HOM by comparison with an authentic standard, showing matching retention time and fragmentation pattern (Supplementary Fig. S7). Together, these results demonstrate that enzyme replacement, rather than point mutagenesis of the native scaffold, was required to expand the accessible flavonoid repertoire in ADP1.

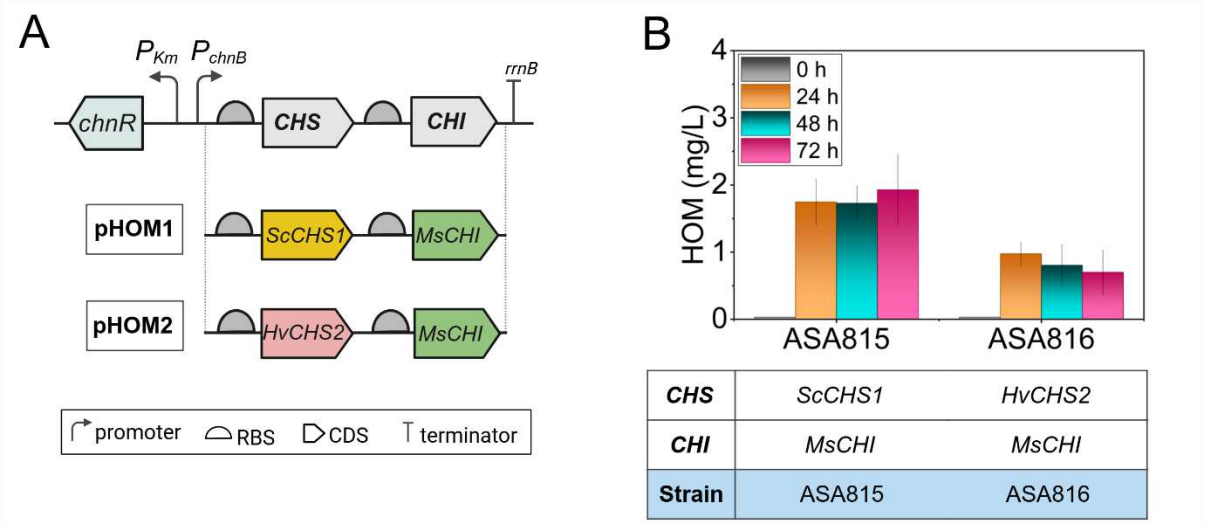


Figure 2. Production of HOM in ADP1. (A) Organization of plasmids carrying *CHS* and *CHI* expression modules from different plant species, (B) Production profile of HOM by ASA815 (Δ*hcaA ScCHS1 MsCHI*) and ASA816 (Δ*hcaA HvCHS2 MsCHI*). Cells were grown in MGC supplemented with 2.5 mM ferulate for 72 h at 30° C. Gene expressions were induced with 0.5 µM cyclohexanone. Data are presented as mean ± standard deviation (s.d.) from three independent biological replicates (n = 3). CHS: chalcone synthase; CHI: chalcone isomerase; Sc: *Stenoloma chusanum*; Hv: *Hordeum vulgare*; Ms: *Medicago sativa*.

Assessment of additional culture parameters for HOM biosynthesis

Though the newly constructed strains were capable of producing HOM, the obtained titers remained low under the initial cultivation conditions. We therefore sought to improve HOM production by evaluating cultivation conditions known to strongly influence flavonoid biosynthesis [20,58,59]. Specifically, we assessed the effects of inoculum size (OD_{600}), ferulate concentration, buffering conditions, inducer concentration, and cultivation temperature. Both strains were included in these analyses to determine whether their production responses differed under altered cultivation conditions.

We first evaluated the effect of inoculum density and ferulate concentration by testing two initial OD_{600} values (0.8 and 2.0) and two substrate concentrations (1 mM and 2.5 mM). As shown in Fig. 2A-2B, reducing ferulate concentration from 2.5 mM to 1 mM consistently improved HOM production in both strains, indicating that elevated precursor loading negatively affected pathway performance. This effect may be attributed to the toxic accumulation of feruloyl-CoA in the *hcaA* deletion strain [60]. In addition, lower inoculum density also favored HOM production, with initial cultivation at OD_{600} 0.8 resulting in higher titers than OD_{600} 2.0 for both constructs. At an initial OD_{600} of 0.8, cultivation with 1 mM ferulate resulted in higher HOM titer than 2.5 mM ferulate in both strains (Fig. 3A, 3B). Under these conditions, ASA815 produced 2.6 mg/L (1.5-fold higher), while ASA816 produced 2.7 mg/L (2.8-fold higher) after 24 h. Furthermore, MOPS supplementation and inducer concentrations had only minor effects on HOM production, indicating that the standard cultivation conditions were largely sufficient for pathway expression (Supplementary Fig. S8-S9). Based on these results, an initial OD_{600} 0.8 and ferulate concentration of 1 mM were selected for subsequent experiments.

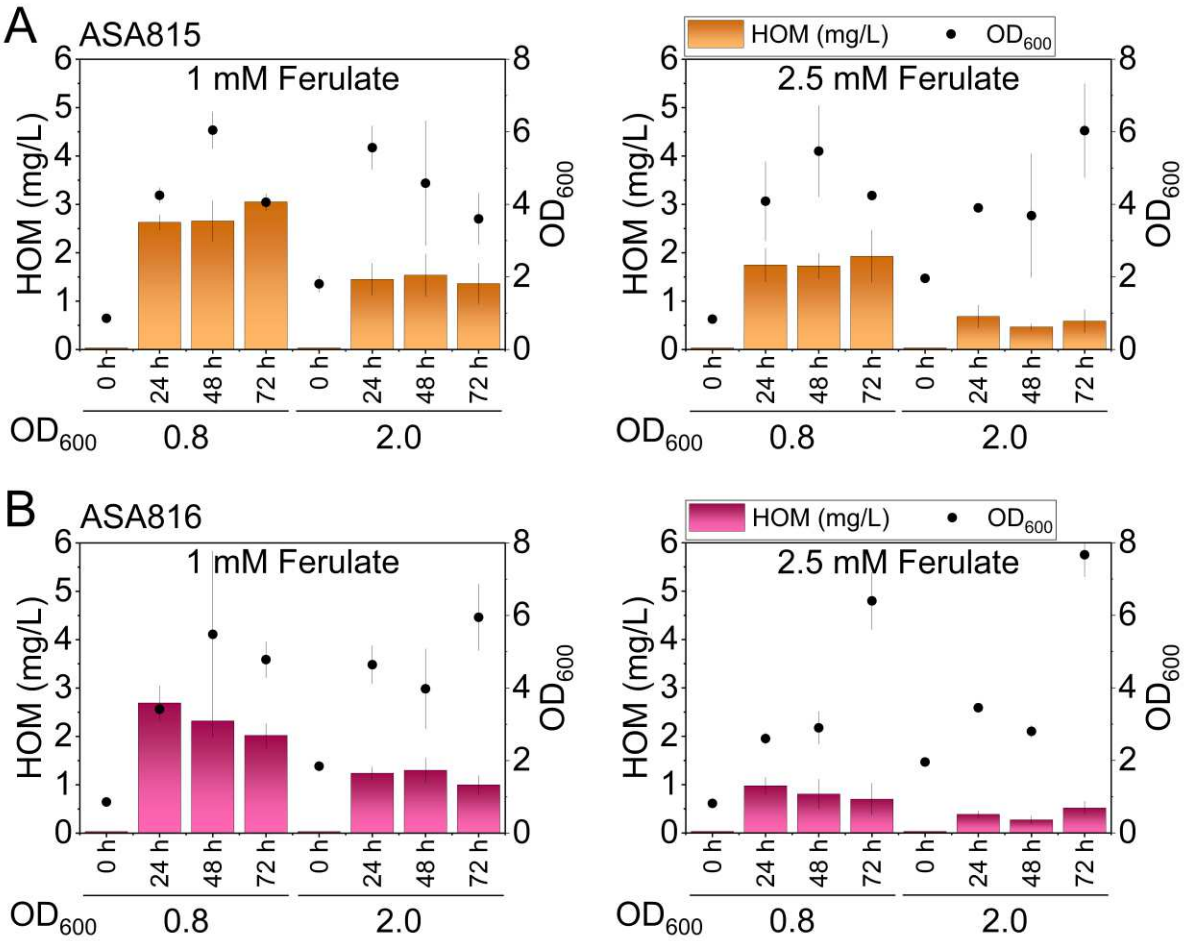
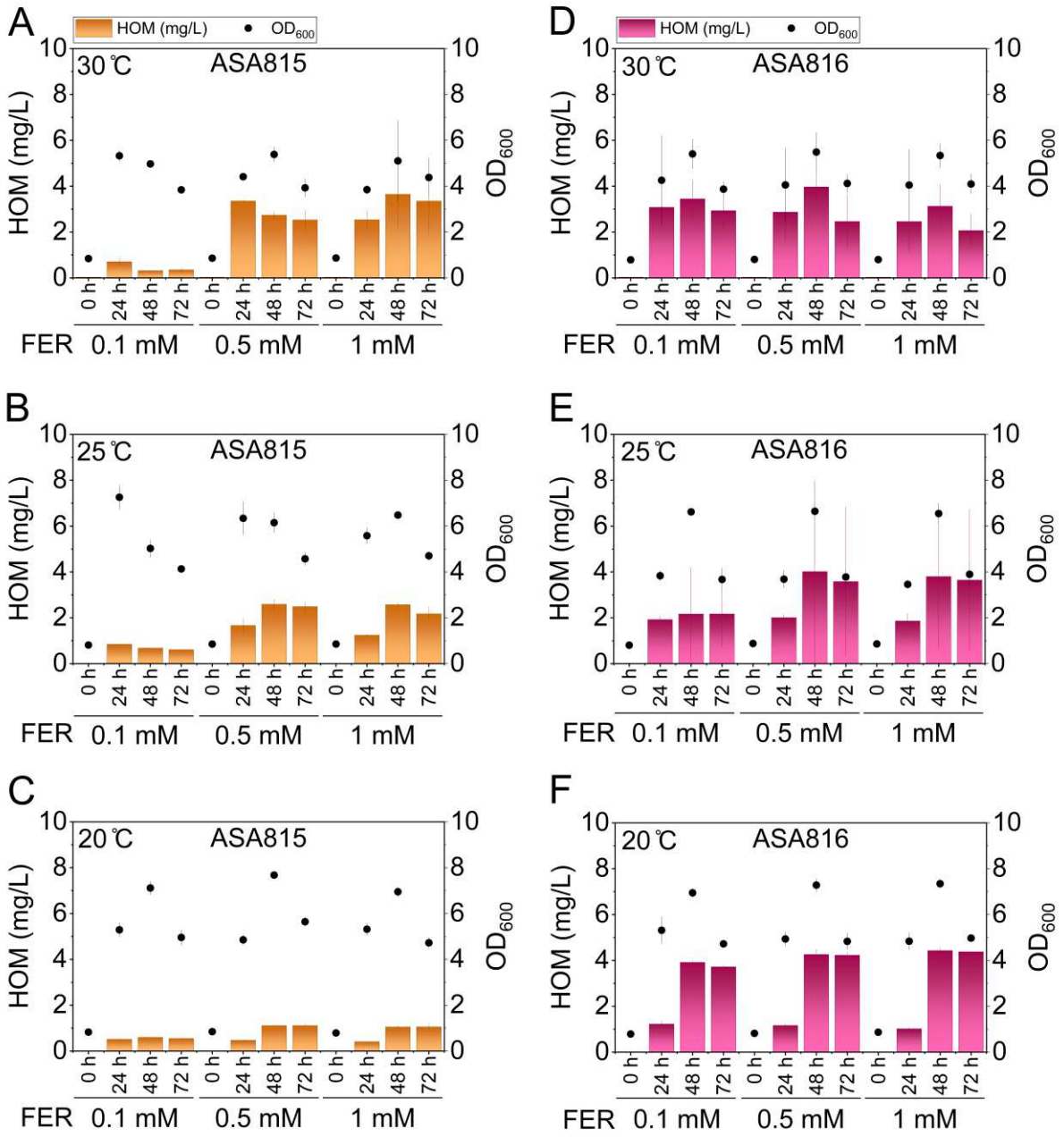


Figure 3. Effect of ferulate concentration and initial cell density (OD_{600}) on HOM production in ADP1. Growth profile and HOM production in (A) ASA815 and (B) ASA816 for 72 h. Cells were cultured in MGC at different ferulate concentrations (1.0 and 2.5 mM) and two initial cell densities (OD_{600} = 0.8 and 2.0). Gene expressions were induced with 0.5 µM cyclohexanone. Data are presented as mean ± standard deviation (s.d.) from three independent biological replicates (n = 3).

Reduced cultivation temperatures have been widely used in flavonoid production studies, particularly in *E. coli* platforms that incorporate a temperature shift during the production phase [8,15,53]. We therefore evaluated HOM production at different temperatures cultivation 20 °C, 25 °C, and 30 °C. In parallel, substrate-loading regimes were further assessed using

ferulate concentrations of 0.1, 0.5, and 1 mM to determine whether production could be maintained at lower precursor inputs (Fig. 4A-4F). As shown in Fig. 4A-4C, ASA815 strain exhibited a pronounced temperature dependence, with the highest HOM titers observed at 30 °C. HOM production by ASA815 was largely unaffected by ferulate concentration between 0.5 and 1 mM, indicating that substrate loading was not limiting within this range. In contrast, ASA816 was less sensitive to cultivation temperature and produced comparable HOM titers across the tested temperature range, including 20 °C (Fig. 4D-4F). While product formation was delayed at lower temperature, the HOM titers remained relatively stable throughout cultivation, suggesting that HOM biosynthesis is favored under these conditions. The ASA816 strain was also showed no significant differences in production between 0.1-1 mM ferulate. Interestingly, the two CHS modules displayed markedly different temperature responses despite being expressed in the same host background, indicating that the choice of CHS substantially influences pathway performance across cultivation conditions. Together, these results reveal distinct cultivation responses between the two CHS module configurations, with ASA816 exhibiting greater tolerance to variations in temperature and precursor availability.



414

415 Figure 4. Effect of temperature cultivation for HOM production in ADP1. (A-C) Growth profile
416 and HOM production in ASA815 at different temperatures (30° C, 25° C, 20° C) for 72 h. (D-F)
417 Growth profile and HOM production in ASA816 at different temperatures (30° C, 25° C, 20° C)
418 for 72 h. Cells were cultured in MGC supplemented with different concentration of ferulate
419 (FER) (0.1, 0.5, and 1 mM). Gene expressions were induced with 0.5 μM cyclohexanone. Data

are presented as mean ± standard deviation (s.d.) from three independent biological replicates (n = 3).

ERI production from caffeate in ADP1

ERI can be synthesized from NAR through flavonoid 3′-hydroxylase (F3′H)-mediated hydroxylation at the 3′ position of the flavonoid B-ring. However, functional expression of this membrane-bound cytochrome P450 enzyme in bacterial hosts remains challenging due to its dependence on cytochrome P450 reductases and associated electron transfer systems [20]. Previous studies therefore employed the native *E. coli* hydroxylase complex HpaBC as a non-P450 alternative for ERI biosynthesis [20]. Alternatively, ERI can also be synthesized directly from caffeate through the CHS–CHI module, thereby bypassing the hydroxylation step and shortening the overall pathway. Motivated by this, we next investigated whether our established platforms could be further extended toward production of an additional flavonoid from a distinct LDA substrate.

ASA815 and ASA816 were cultivated under their respective optimized conditions for HOM production and supplied with varying concentrations of caffeate. ASA815 supported substantial ERI production, reaching 24.2 mg/L at 0.5 mM caffeate, whereas ASA816 produced only trace amounts (<5 mg/L) across the tested aromatic concentrations (Fig. 5A-5B). Notably, ERI production by ASA815 exceeded the HOM titers obtained under the same cultivation framework, indicating that caffeate may be a more favorable substrate for pathway extension in this configuration. These findings demonstrate that aromatic precursor substitution is sufficient to redirect flavonoid biosynthesis while retaining the same downstream CHS–CHI module. The marked difference between ASA815 and ASA816 further indicates that pathway

configuration influences not only production performance but also the accessible flavonoid product spectrum.

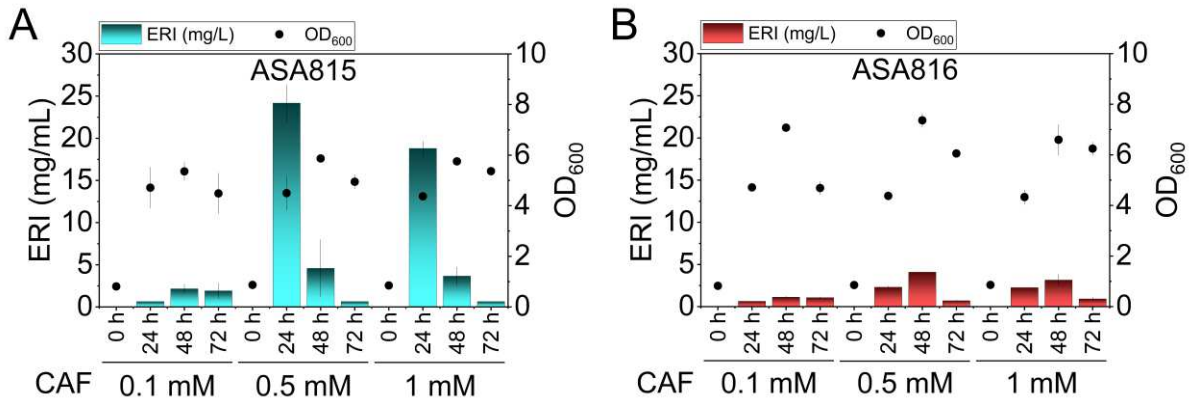


Figure 5. Production of ERI by ADP1 from caffeate. (A), (B) Growth profile and ERI production in ASA815 and ASA816. Cells were grown in MGC supplemented with different concentrations of caffeate (CAF) (0.1, 0.5, and 1 mM) for 72 h. Gene expressions were induced with 0.5 μM cyclohexanone. ASA815 strain was cultivated at 30 °C, whereas ASA816 was cultivated at 20 °C. Data are presented as mean ± standard deviation (s.d.) from three independent biological replicates (n = 3).

Multi-flavonoid production in Fed-batch bioreactor

In our previous study, fed-batch cultivation improved NAR production from *p*-coumarate by the engineered ADP1 strain [13]. Based on this result, we applied the same cultivation strategy to evaluate strain performance with mixed aromatic substrates. Fed-batch cultivation was performed in a 250-mL bioreactor, with 1 mM each of ferulate, caffeate, and *p*-coumarate supplied at a feeding rate of 3.7 mL/h for 48 h (Fig. 6A). Samples were collected throughout cultivation monitor optical density (OD_{600}), aromatic substrate concentrations, and flavonoid production. Notably, the culture broth gradually changed from light to dark brown after

approximately 24 h of cultivation, consistent with oxidative transformation of caffeate under aerobic conditions.

ASA815 supported production of all three target flavonoids, with the highest accumulation observed for NAR (8.1 mg/L) and the lowest for HOM (1.3 mg/L) after 54 h cultivation (Fig. 6B). In contrast, ASA816 displayed narrower product profile, producing predominantly HOM (3.2 mg/L), with no detectable formation of NAR and ERI after 60 h (Fig. 6C). Unexpectedly, mixed-aromatic fed-batch cultivation did not improve flavonoid titers relative to flask cultivations supplied with individual aromatic substrates. This reduction in productivity may be associated with the simultaneous conversion of three aromatic precursors, potentially due to increased metabolic demand or competition for shared pathway precursors such as malonyl-CoA, which serves as the extender unit for flavonoid biosynthesis [15,20]. Together, these results indicate that ASA815 carrying *ScCHS1* supports broader flavonoid diversification under mixed-aromatic feeding, whereas ASA816 carrying *HvCHS2* displays a more selective production profile.

Given the lower flavonoid titers obtained during mixed-aromatic fed-batch cultivation, we next examined whether reducing the total aromatic concentration could improve pathway performance. Due to its broader flavonoid product profile, ASA815 was selected and cultivated with medium supplemented with lower aromatic loading (0.5 mM each of ferulate, caffeate, and *p*-coumarate). The strain resulted in a modest increase of NAR and ERI by 1.3-fold and 2.0-fold, respectively, whereas HOM production remained largely unchanged (Supplementary Fig. S10). This observation supports the notion that elevated aromatic loading may contribute to reduced flavonoid productivity under mixed-substrate conditions.

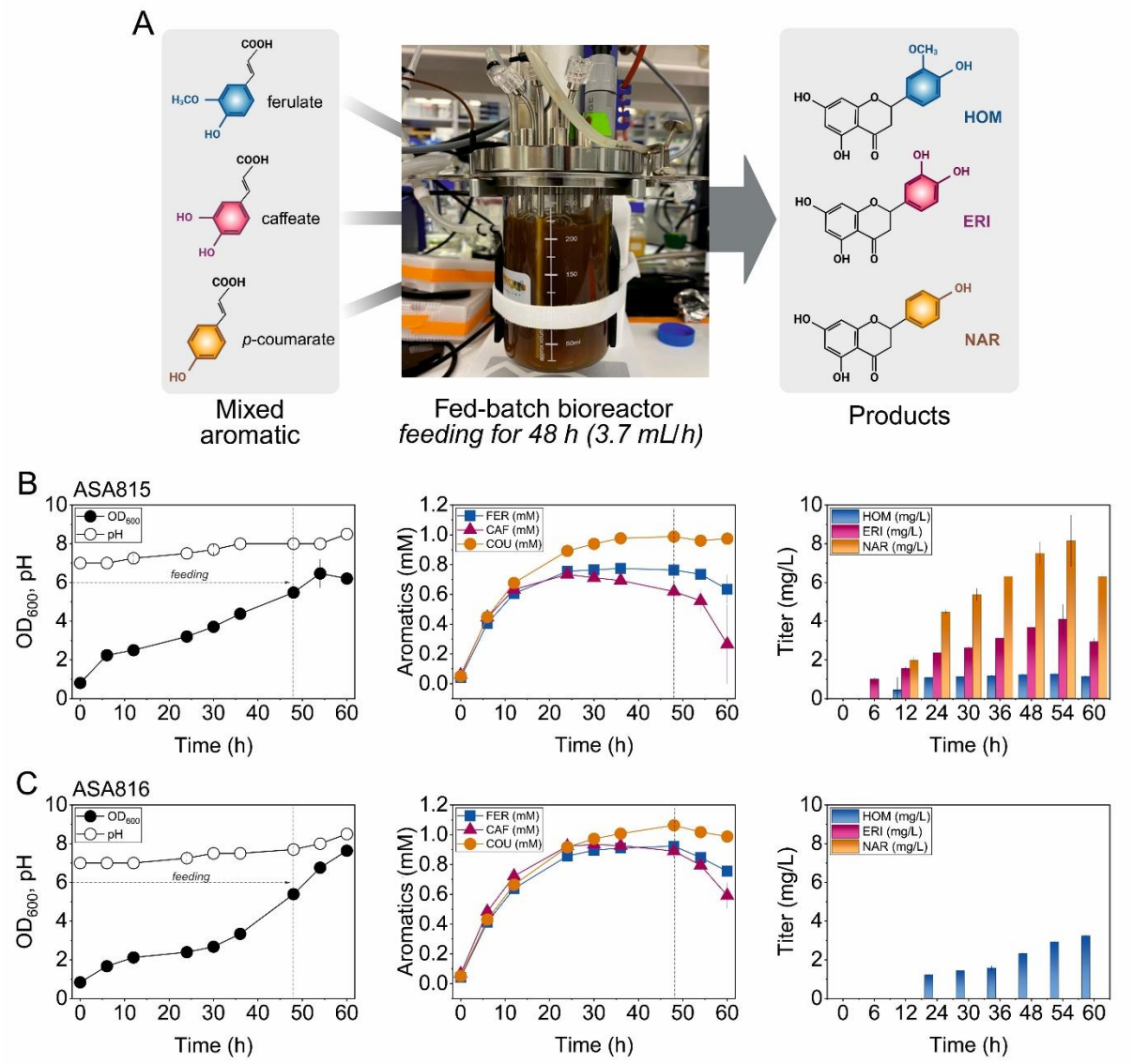


Figure 6. Production of multiple flavonoids (HOM, ERI, NAR) from aromatics mixture (ferulate, caffeate, and *p*-coumarate) in fed-batch cultivation. (A) Fed-batch bioreactor used for cultivation of the engineered ADP1 strains, (B), (C) Time course profiles of OD_{600} profile, aromatics consumption, and flavonoid production by ASA815 and ASA816. Cells were cultured in MGC with 1 mM ferulate, 1 mM caffeate, and 1 mM *p*-coumarate. Gene expressions were induced with 0.5 μM cyclohexanone. ASA815 strain was cultivated at 30 °C, whereas ASA816 was cultivated at 20 °C. Feeding was added from 0-48 h, at flow rate 3.5 mL/h. Data are presented as mean ± standard deviation (s.d.) from two independent biological replicates (n = 2). HPLC profile of NAR, HOM, and ERI are provided in Supplementary Fig. S11.

Multi-flavonoid production from APL

Having established flavonoid production from defined aromatic substrates, we next evaluated whether the platform could operate directly on APLs derived from lignocellulosic biomass. Wheat straw and organosolv lignin APLs were selected to assess whether flavonoid production could be achieved across lignin-derived streams. Wheat straw and straw-derived organosolv lignin were subjected to alkaline depolymerization at 130 °C using 70 mg NaOH per g dry biomass and 2% NaOH (w/w), respectively, followed by centrifugation and filtration. HPLC analysis revealed that the wheat straw APL contained approximately 2.2 mM *p*-coumarate and 1.1 mM ferulate, whereas the organosolv lignin APL contained 4.7 mM *p*-coumarate and 5.0 mM ferulate. In contrast, caffeate was not detected in either APL (Fig. 7A).

We subsequently evaluated the ability of ASA815 to produce flavonoids directly from APL. To enable direct comparison between feedstocks, wheat straw and organosolv lignin APLs were supplemented at equivalent aromatic loadings corresponding to 0.5 mM *p*-coumarate and cultivated in shake flasks containing MGC for 72 h. Under these conditions, strain ASA815 produced NAR and HOM (Fig. 7B), demonstrating that the heterologous pathway remained functional in complex lignin-derived substrate mixtures. In addition, no adverse effects on growth were observed in the presence of either wheat straw- or organosolv lignin APL (Supplementary Fig. S12), indicating that the liquors were well tolerated under the tested conditions. Collectively, these results demonstrate that ADP1 can convert heterogeneous LDA streams into flavonoid products, highlighting its potential as a chassis for the production of high-value plant natural products from renewable biomass feedstocks.

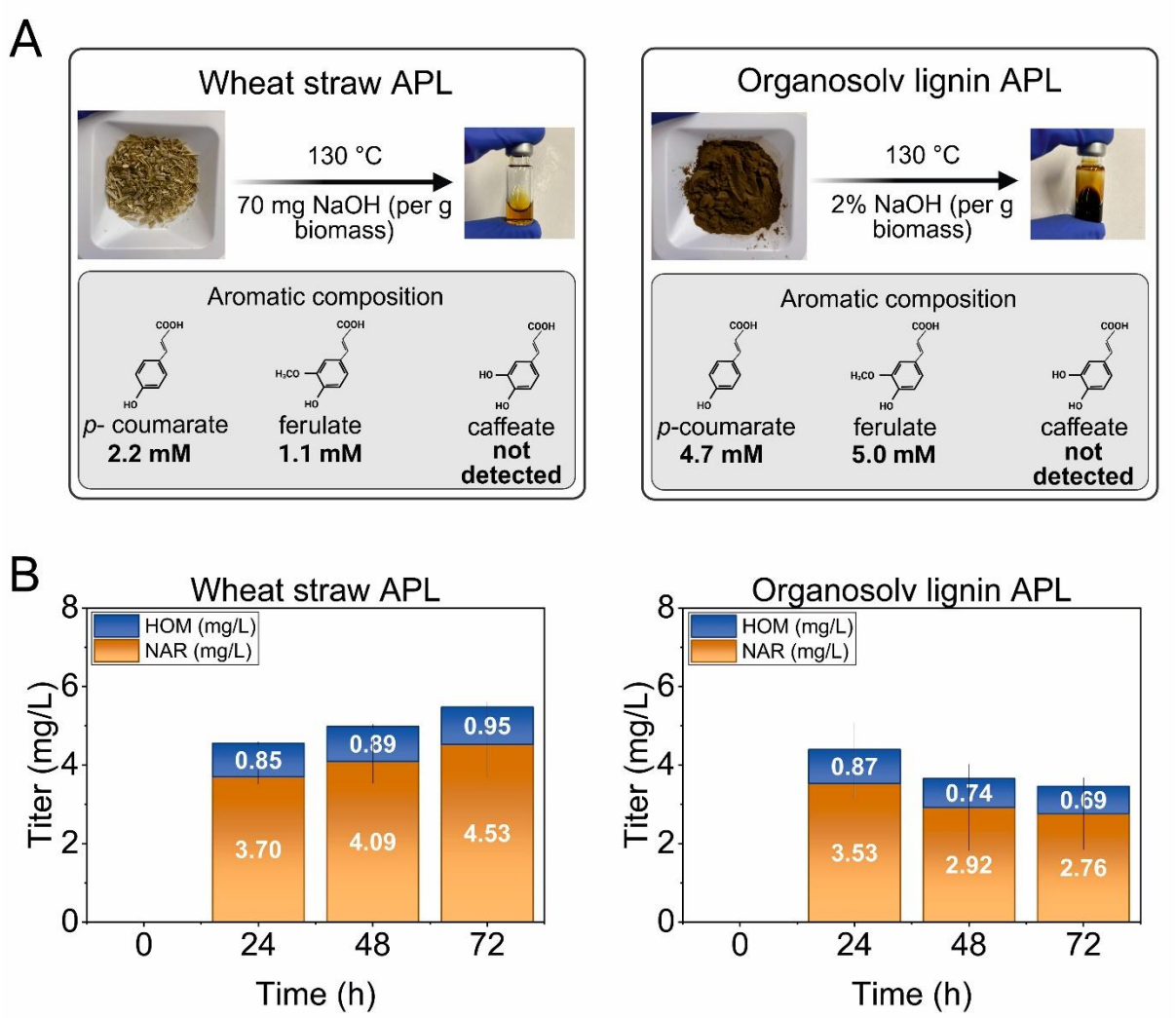


Figure 7. Flavonoid production from APLs. (A) Preparation of alkaline pretreated liquor (APL) from wheat straw and organosolv lignin, and aromatic concentration measured by HPLC. (B) Flavonoid production from wheat-straw and organosolv lignin by ASA815. Cells were cultivated in MGC supplemented with APLs at an equivalent aromatic loading corresponding to 0.5 mM *p*-coumarate. Gene expression was induced with 0.5 μM cyclohexanone. Data are presented as mean ± standard deviation (s.d.) from three independent biological replicates (n = 3).

Discussion

In this study, we expanded flavonoid biosynthesis in ADP1 beyond NAR by extending the precursor scope from *p*-coumarate to ferulate and caffeate, enabling the production of structurally distinct flavonoids from different LDAs. Through *CHS* ortholog selection and cultivation optimization, the best-performing strain (ASA815) achieved titers of 3.7 mg/L HOM and 24.2 mg/L ERI in flask cultivations. These results position ADP1 not only as a host for single-product flavonoid synthesis, but as a promising platform for converting diverse LDAs into value-added flavonoids.

CHS generally exhibit a strong preference for *p*-coumaroyl-CoA as a starter substrate, which underlies their widespread use in NAR biosynthesis [61]. This substrate preference presented a key challenge when extending the ADP1 platform from *p*-coumarate-derived NAR to flavonoids derived from alternative aromatic precursors. We initially sought to overcome this limitation by rationally modifying CHS substrate specificity; however, none of the three variants tested supported detectable production of the target compounds. Rather than being restricted to *p*-coumaroyl-CoA utilization, however, some naturally occurring *CHS*s exhibit broader or altered starter-substrate preferences. For example, an *HvCHS2* has been identified as a variant with HOM/ERI synthase activity [62]. Similarly, a *ScCHS1* was recently reported to exhibit preference for feruloyl-CoA, enabling HOM production in *E. coli* [53]. Although such activities appear uncommon among characterized *CHS*s, their occurrence suggested that natural *CHS* diversity could provide an alternative route to the desired substrate specificity. Consistent with this, screening of *CHS* orthologs in our study identified enzymes that enabled HOM production, whereas this activity was not detected among the three rationally engineered variants tested.

Despite being expressed in an identical metabolic background, the two *CHS* variants exhibited distinct flavonoid production profiles, highlighting intrinsic differences in enzyme performance. The effect of cultivation parameters was also variant-dependent, as changes in temperature and precursor loading altered the relative performance of the two constructs. While enzyme screening studies often identify a single superior variant under a specific cultivation condition [12,63], our results indicate that *CHS* performance is highly condition-dependent, with each ortholog exhibiting advantages under different operating conditions. In addition, we cannot exclude the possibility that certain variants may channel intermediates toward alternative products that were not detected or resolved in the present analysis. Previous studies have shown that *CHS* can generate competing pyrone by-products through alternative cyclization pathways and that chalcone isomerase-like proteins (CHILs) can enhance flavonoid production by suppressing these metabolic shunts and redirecting flux toward the desired products [64,65]. Consistent with this, Ni et al. (2022) reported the formation of BNY-type and CTAL-type pyrone derivatives when feruloyl-CoA was used as a starter substrate [53]. Together, these findings indicate that no single cultivation condition is universally optimal and that maximizing flavonoid production requires aligning enzyme-specific characteristics and flux-partitioning behavior with appropriate process conditions.

In bioreactor cultivations containing aromatic mixtures, the engineered ADP1 strain produced multiple flavonoids, demonstrating its ability to convert diverse LDAs into distinct products. Previous microbial flavonoid production studies have predominantly focused on the synthesis of individual flavonoids from defined substrates [12,53], whereas our approach enables simultaneous generation of multiple flavonoid products from mixed aromatic feedstocks. Although our flavonoid titers were lower than those obtained from individual substrates, aromatic mixtures more closely resemble the heterogeneous composition of lignin-derived

574 feedstocks encountered in industrial biorefineries. Importantly, the ability to generate different
575 flavonoids from their corresponding aromatic precursors without further genetic modification
576 demonstrates the product flexibility of the engineered platform and provides a basis for its
577 application to heterogeneous lignin-derived streams.

578 The lower flavonoid production observed with the aromatic mixture may arise from several
579 factors associated with simultaneous substrate conversion. Competition for shared pathway
580 precursors, including malonyl-CoA, could limit flux when multiple flavonoid pathways operate
581 concurrently [17]. In addition, accumulation of aromatic intermediates or CoA-activated
582 derivatives may impose metabolic burden and toxicity [13,66,66], further constraining
583 flavonoid production. However, as these factors were not directly investigated in the present
584 study, the mechanisms underlying the reduced production remain to be determined.

585 Importantly, flavonoid production was also achieved directly from wheat straw- and
586 organosolv lignin APLs, demonstrating the functionality of the pathway in complex and
587 industrially relevant feedstocks. APL has previously been used as a substrate for microbial
588 production such as medium-chain-length polyhydroxyalkanoates (*mcl*-PHAs) in *Pseudomonas*
589 *putida* KT2440 [35]. More recently, vanillin-glucoside and resveratrol were produced from a
590 synthetic mock APL using *A. baylyi* ADP1 [67]. However, direct flavonoid production from
591 lignin-derived process streams remains largely unexplored. Thus, production from two
592 compositionally distinct APLs extends the range of product accessible from LDAs and
593 highlights the potential of ADP1 to accommodate variation in complex lignin streams. Notably,
594 production was achieved despite the potential presence of inhibitory or unidentified
595 compounds in these streams.

Together, this study expands flavonoid biosynthesis in ADP1 beyond NAR and establishes its ability to convert multiple LDA precursors into structurally distinct flavonoids. While the titers remain below those achieved in highly optimized sugar-based *E. coli* [8,53,68] and yeast systems [69], the significance of this work lies in a fundamentally different production paradigm; rather than reconstructing aromatic precursor pathways from glucose, ADP1 directly exploits LDAs as pathway entry points, enabling substrate-directed production of NAR, ERI, and HOM within a single engineered host. Importantly, this functionality was maintained in complex lignin-derived liquors, demonstrating robustness toward heterogeneous feedstocks and providing a direct link between lignin valorization and flavonoid biosynthesis. These findings position ADP1 as a versatile chassis for transforming renewable aromatic side streams into high-value products and establish a foundation for more efficient lignin-based biomanufacturing.

Conclusion

We demonstrated the production of multiple flavonoids in ADP1 from LDAs. Through identification of an effective CHS-CHI enzyme combination and optimization of cultivation conditions, the engineered strain produced 3.7 mg/L HOM and 24.2 mg/L ERI in flask cultivations. In addition to expanding flavonoid biosynthesis in ADP1 beyond NAR, this work demonstrates a distinct production strategy in which LDAs, including ferulate, caffeate, and *p*-coumarate, serve as direct biosynthetic precursors for structurally diverse flavonoids. Importantly, a single engineered strain enabled substrate-directed production of NAR, ERI, and HOM through feedstock selection without additional genetic modifications. Furthermore, the flavonoid production was maintained directly from APLs, demonstrating compatibility with

complex and industrially relevant lignin-derived feedstock. Together, these results position ADP1 as a promising host for lignin valorization and establish a foundation for a substrate-driven flavonoid production, in which lignin-derived precursors are directly funneled into diverse flavonoid products using a single microbial chassis.

Acknowledgments

We thank Jin Luo and Haochen Sun for their assistance with APL preparation. Schematic figures were created with BioRender.com.

Funding

This work was supported by the Novo Nordisk Foundation [NNF21OC0067758 to S.S., NNF21OC0079579 to V.S.]; the Research Council of Finland (RCF) [347204, 353587, and 372132 to S.S.]. This research was also supported by FIN-BioFoundry (RCF, grant no. 367615) and from the European Union – NextGenerationEU instrument, funded by the Research Council of Finland under grant number 353658.

Author information

Authors and Affiliations

Faculty of Engineering and Natural Sciences, Tampere University, Hervanta Campus, PO Box 527, Tampere, FI-33014, Finland

Kesi Kurnia, Aarni Mäkelä, Elena Efimova, Ville Santala & Suvi Santala

Faculty of Medicine and Health Technology, Tampere University, Kauppi Campus, Arvo Ylpön katu 34, Tampere, FI-33520, Finland

Vasyl V. Mykuliak & Vesa P. Hytönen

Fimlab Laboratories, Arvo Ylpön katu 4, Tampere, FI-33520, Finland

Vesa P. Hytönen

Contributions

KK, VS, and SS conceived and designed the study. KK performed the experiments, analyzed the data, and drafted the manuscript. AM contributed to plasmid and strain construction. EE contributed to HPLC and LC-MS analysis. VM contributed to the design of protein mutations targeting enzyme activity. VH, VS, and SS supervised the study and secured resources. All authors participated in writing and reviewing the manuscript. All authors read, edited, and approved the final manuscript.

Competing interests

The authors declare that they have no conflict of interest.

References

1. Panche AN, Diwan AD, Chandra SR. Flavonoids: an overview. J Nutr Sci. 2016;5:e47. https://doi.org/10.1017/jns.2016.41

2. Pandey RP, Parajuli P, Koffas MAG, Sohng JK. Microbial production of natural and non-natural flavonoids: Pathway engineering, directed evolution and systems/synthetic biology. Biotechnology Advances. 2016;34:634–62. https://doi.org/10.1016/j.biotechadv.2016.02.012

3. Duarte M, Pedrosa SS, Khusial PR, Madureira AR. The biological potential and health-benefits of flavonoids: A review and development opportunities. Chemico-Biological Interactions. 2025;421:111755. https://doi.org/10.1016/j.cbi.2025.111755

4. Peng B, Dai L, Iacovelli R, Driessen AJM, Haslinger K. Heterologous Naringenin Production in the Filamentous Fungus *Penicillium rubens*. J Agric Food Chem. 2023;71:20782–92. https://doi.org/10.1021/acs.jafc.3c06755

5. Jomova K, Alomar SY, Valko R, Liska J, Nepovimova E, Kuca K, et al. Flavonoids and their role in oxidative stress, inflammation, and human diseases. Chemico-Biological Interactions. 2025;413:111489. https://doi.org/10.1016/j.cbi.2025.111489

6. Tutunchi H, Naeini F, Ostadrahimi A, Hosseinzadeh-Attar MJ. Naringenin, a flavanone with antiviral and anti-inflammatory effects: A promising treatment strategy against COVID -19. Phytotherapy Research. 2020;34:3137–47. https://doi.org/10.1002/ptr.6781

7. Koirala N, Thuan NH, Ghimire GP, Thang DV, Sohng JK. Methylation of flavonoids: Chemical structures, bioactivities, progress and perspectives for biotechnological production. Enzyme and Microbial Technology. 2016;86:103–16. https://doi.org/10.1016/j.enzmictec.2016.02.003

8. Peng B, Zhang L, He S, Oerlemans R, Quax WJ, Groves MR, et al. Engineering a Plant Polyketide Synthase for the Biosynthesis of Methylated Flavonoids. J Agric Food Chem. 2024;72:529–39. https://doi.org/10.1021/acs.jafc.3c06785

9. Koopman F, Beekwilder J, Crimi B, Van Houwelingen A, Hall RD, Bosch D, et al. De novo production of the flavonoid naringenin in engineered *Saccharomyces cerevisiae*. Microb Cell Fact. 2012;11:155. https://doi.org/10.1186/1475-2859-11-155

10. Ye S, Magadán-Corpas P, Pérez-Valero Á, Villar CJ, Lombó F. Metabolic engineering strategies for naringenin production enhancement in *Streptomyces albidoflavus* J1074. Microb Cell Fact. 2023;22:167. https://doi.org/10.1186/s12934-023-02172-5

11. Hwang HG, Noh MH, Koffas MAG, Jang S, Jung GY. Multi-level rebalancing of the naringenin pathway using riboswitch-guided high-throughput screening. Metabolic Engineering. 2021;67:417–27. https://doi.org/10.1016/j.ymben.2021.08.003

12. Dunstan MS, Robinson CJ, Jervis AJ, Yan C, Carbonell P, Hollywood KA, et al. Engineering Escherichia coli towards de novo production of gatekeeper (2S)-flavanones: naringenin, pinocembrin, eriodictyol and homoeriodictyol. Synthetic Biology. 2020;5:ysaa012. https://doi.org/10.1093/synbio/ysaa012

13. Kurnia K, Efimova E, Santala V, Santala S. Metabolic engineering of *Acinetobacter baylyi* ADP1 for naringenin production. Metabolic Engineering Communications. 2024;19:e00249. https://doi.org/10.1016/j.mec.2024.e00249

14. Hwang HG, Milito A, Yang J-S, Jang S, Jung GY. Riboswitch-guided chalcone synthase engineering and metabolic flux optimization for enhanced production of flavonoids. Metabolic Engineering. 2023;75:143–52. https://doi.org/10.1016/j.ymben.2022.12.006

15. Zhou S, Yuan S-F, Nair PH, Alper HS, Deng Y, Zhou J. Development of a growth coupled and multi-layered dynamic regulation network balancing malonyl-CoA node to enhance (2S)-naringenin biosynthesis in Escherichia coli. Metabolic Engineering. 2021;67:41–52. https://doi.org/10.1016/j.ymben.2021.05.007

16. Gao S, Lyu Y, Zeng W, Du G, Zhou J, Chen J. Efficient Biosynthesis of (2 *S*)-Naringenin from *p* -Coumaric Acid in *Saccharomyces cerevisiae*. J Agric Food Chem. 2020;68:1015–21. https://doi.org/10.1021/acs.jafc.9b05218

17. Mao J, Mohedano MT, Fu J, Li X, Liu Q, Nielsen J, et al. Fine-tuning of *p*-coumaric acid synthesis to increase (2S)-naringenin production in yeast. Metabolic Engineering. 2023;79:192–202. https://doi.org/10.1016/j.ymben.2023.08.003

18. Wu J, Zhou T, Du G, Zhou J, Chen J. Modular Optimization of Heterologous Pathways for De Novo Synthesis of (2S)-Naringenin in *Escherichia coli*. Cirino PC, editor. PLoS ONE. 2014;9:e101492. https://doi.org/10.1371/journal.pone.0101492

19. Liu D, Sica MS, Mao J, Chao LF-I, Siewers V. A *p* -Coumaroyl-CoA Biosensor for Dynamic Regulation of Naringenin Biosynthesis in *Saccharomyces cerevisiae*. ACS Synth Biol. 2022;11:3228–38. https://doi.org/10.1021/acssynbio.2c00111

20. Wu X, Liu J, Liu D, Yuwen M, Koffas MAG, Zha J. Biosynthesis of eriodictyol from tyrosine by *Corynebacterium glutamicum*. Microb Cell Fact. 2022;21:86. https://doi.org/10.1186/s12934-022-01815-3

21. Wu X, Yuwen M, Pu Z, Zhao Z, Yu H, Zha J. Engineering of flavonoid 3′-O-methyltransferase for improved biosynthesis of chrysoeriol in *Escherichia coli*. Appl Microbiol Biotechnol. 2023;107:1663–72. https://doi.org/10.1007/s00253-023-12403-9

22. Becker J, Wittmann C. A field of dreams: Lignin valorization into chemicals, materials, fuels, and health-care products. Biotechnology Advances. 2019;37:107360. https://doi.org/10.1016/j.biotechadv.2019.02.016

23. Weiland F, Kohlstedt M, Wittmann C. Guiding stars to the field of dreams: Metabolically engineered pathways and microbial platforms for a sustainable lignin-based industry. Metabolic Engineering. 2022;71:13–41. https://doi.org/10.1016/j.ymben.2021.11.011

24. Jiju PS, Patel AK, Shruthy NS, Shalu S, Dong C-D, Singhania RR. Sustainability through lignin valorization: recent innovations and applications driving industrial transformation. Bioresour Bioprocess. 2025;12:88. https://doi.org/10.1186/s40643-025-00929-x

25. Boudet A-M. A new view of lignification. Trends in Plant Science. 1998;3:67–71. https://doi.org/10.1016/S1360-1385(97)01176-X

26. Yu X, Yang B, Zhu W, Deng T, Pu Y, Ragauskas A, et al. Towards functionalized lignin and its derivatives for high-value material applications. Industrial Crops and Products. 2023;200:116824. https://doi.org/10.1016/j.indcrop.2023.116824

27. Bruijnincx PCA, Rinaldi R, Weckhuysen BM. Unlocking the potential of a sleeping giant: lignins as sustainable raw materials for renewable fuels, chemicals and materials. Green Chem. 2015;17:4860–1. https://doi.org/10.1039/C5GC90055G

28. Bajwa DS, Pourhashem G, Ullah AH, Bajwa SG. A concise review of current lignin production, applications, products and their environmental impact. Industrial Crops and Products. 2019;139:111526. https://doi.org/10.1016/j.indcrop.2019.111526

29. Balakshin MYu, Capanema EA, Sulaeva I, Schlee P, Huang Z, Feng M, et al. New Opportunities in the Valorization of Technical Lignins. ChemSusChem. 2021;14:1016–36. https://doi.org/10.1002/cssc.202002553

30. Li F, Zhao Y, Xue L, Ma F, Dai SY, Xie S. Microbial lignin valorization through depolymerization to aromatics conversion. Trends in Biotechnology. 2022;40:1469–87. https://doi.org/10.1016/j.tibtech.2022.09.009

31. Zhang X-L, Liu Z-H, Li B-Z, Yuan Y-J. Tapping into the natural aromatic potential of microbial lignin valorization towards aromatic fine chemicals. Green Chem. 2024;26:11378–405. https://doi.org/10.1039/D4GC03567D

32. Sodré V, Bugg TDH. Sustainable production of aromatic chemicals from lignin using enzymes and engineered microbes. Chem Commun. 2024;60:14360–75. https://doi.org/10.1039/D4CC05064A

33. Becker J, Kuhl M, Kohlstedt M, Starck S, Wittmann C. Metabolic engineering of *Corynebacterium glutamicum* for the production of *cis, cis*-muconic acid from lignin. Microb Cell Fact. 2018;17:115. https://doi.org/10.1186/s12934-018-0963-2

34. Arvay E, Biggs BW, Guerrero L, Jiang V, Tyo K. Engineering *Acinetobacter baylyi* ADP1 for mevalonate production from lignin-derived aromatic compounds. Metabolic Engineering Communications. 2021;13:e00173. https://doi.org/10.1016/j.mec.2021.e00173

35. Linger JG, Vardon DR, Guarnieri MT, Karp EM, Hunsinger GB, Franden MA, et al. Lignin valorization through integrated biological funneling and chemical catalysis. Proc Natl Acad Sci USA. 2014;111:12013–8. https://doi.org/10.1073/pnas.1410657111

36. Lan H-N, Liu R-Y, Liu Z-H, Li X, Li B-Z, Yuan Y-J. Biological valorization of lignin to flavonoids. Biotechnology Advances. 2023;64:108107. https://doi.org/10.1016/j.biotechadv.2023.108107

37. Jiang H, Wood KV, Morgan JA. Metabolic Engineering of the Phenylpropanoid Pathway in *Saccharomyces cerevisiae*. Appl Environ Microbiol. 2005;71:2962–9. https://doi.org/10.1128/AEM.71.6.2962-2969.2005

38. Zhou S, Lyu Y, Li H, Koffas MAG, Zhou J. Fine-tuning the (2 *S*)-naringenin synthetic pathway using an iterative high-throughput balancing strategy. Biotech & Bioengineering. 2019;116:1392–404. https://doi.org/10.1002/bit.26941

771 39. Wilkes RA, Borchert AJ, Garcia VE, Geiselman GM, Liu S, Guss AM, et al. Comparison of
772 microbial strains as candidate hosts and genetic reservoirs for the valorization of lignin
773 streams. Green Chem. 2024;26:12053–69. https://doi.org/10.1039/D4GC03876B

774 40. Barbe V. Unique features revealed by the genome sequence of *Acinetobacter* sp. ADP1, a
775 versatile and naturally transformation competent bacterium. Nucleic Acids Research.
776 2004;32:5766–79. https://doi.org/10.1093/nar/gkh910

777 41. Young DM, Parke D, Ornston LN. Opportunities for genetic investigation afforded by
778 *Acinetobacter baylyi*, a nutritionally versatile bacterial species that is highly competent for
779 natural transformation. Annu Rev Microbiol. 2005;59:519–51.
780 https://doi.org/10.1146/annurev.micro.59.051905.105823

781 42. Salmela M, Lehtinen T, Efimova E, Santala S, Santala V. Alkane and wax ester production
782 from lignin-related aromatic compounds. Biotech & Bioengineering. 2019;116:1934–45.
783 https://doi.org/10.1002/bit.27005

784 43. De Vries J, Wackernagel W. Integration of foreign DNA during natural transformation of
785 *Acinetobacter* sp. by homology-facilitated illegitimate recombination. Proc Natl Acad Sci USA.
786 2002;99:2094–9. https://doi.org/10.1073/pnas.042263399

787 44. Santala S, Santala V. *Acinetobacter baylyi* ADP1—naturally competent for synthetic biology.
788 Mattanovich D, Ivan Nikel P, editors. Essays in Biochemistry. 2021;65:309–18.
789 https://doi.org/10.1042/EBC20200136

790 45. Bedore SR, Neidle EL, Pardo I, Luo J, Baugh AC, Duscent-Maitland CV, et al. Natural
791 transformation as a tool in *Acinetobacter baylyi*: Streamlined engineering and mutational
792 analysis. Methods in Microbiology [Internet]. Elsevier; 2023 [cited 2024 Apr 5]. p. 207–34.
793 https://doi.org/10.1016/bs.mim.2023.01.002

794 46. Luo J, McIntyre EA, Bedore SR, Santala V, Neidle EL, Santala S. Characterization of Highly
795 Ferulate-Tolerant *Acinetobacter baylyi* ADP1 Isolates by a Rapid Reverse Engineering Method.
796 Kivisaar M, editor. Appl Environ Microbiol. 2022;88:e01780-21.
797 https://doi.org/10.1128/AEM.01780-21

798 47. Kurnia K, Gifford I, Santala V, Barrick JE, Santala S. Dual-Chassis Strategy for Bridging
799 Adaptive Evolution and Rational Design for Synthetic Biology [Internet]. Synthetic Biology;
800 2026 [cited 2026 June 14]. https://doi.org/10.64898/2026.06.02.729570

801 48. Liu C, Juvonen V, Meriläinen E, Efimova E, Luo J, Salmela M, et al. *Cis,cis*-muconic acid
802 production from lignin related molecules by *Acinetobacter baylyi* ADP1. Microb Cell Fact.
803 2025;24:150. https://doi.org/10.1186/s12934-025-02780-3

804 49. Tuomela H, Koivisto J, Efimova E, Santala S. Conversion and upgrading of syringate by
805 *Acinetobacter baylyi* ADP1. Microb Cell Fact. 2025;24:209. https://doi.org/10.1186/s12934-025-
806 02839-1

807 50. Madeira F, Madhusoodanan N, Lee J, Eusebi A, Niewielska A, Tivey ARN, et al. The EMBL-
808 EBI Job Dispatcher sequence analysis tools framework in 2024. Nucleic Acids Research.
809 2024;52:W521–5. https://doi.org/10.1093/nar/gkae241

810 51. Berezin C, Glaser F, Rosenberg J, Paz I, Pupko T, Fariselli P, et al. ConSeq: the identification
811 of functionally and structurally important residues in protein sequences. Bioinformatics.
812 2004;20:1322–4. https://doi.org/10.1093/bioinformatics/bth070

813 52. Genee HJ, Bonde MT, Bagger FO, Jespersen JB, Sommer MOA, Wernersson R, et al.
814 Software-Supported USER Cloning Strategies for Site-Directed Mutagenesis and DNA
815 Assembly. ACS Synth Biol. American Chemical Society; 2015;4:342–9.
816 https://doi.org/10.1021/sb500194z

817 53. Ni R, Niu M, Fu J, Tan H, Zhu T, Zhang J, et al. Molecular and structural characterization of
818 a promiscuous chalcone synthase from the fern species *Stenoloma chusanum*. JIPB.
819 2022;64:1935–51. https://doi.org/10.1111/jipb.13335

820 54. Luo J, Lehtinen T, Efimova E, Santala V, Santala S. Synthetic metabolic pathway for the
821 production of 1-alkenes from lignin-derived molecules. Microb Cell Fact. 2019;18:48.
822 https://doi.org/10.1186/s12934-019-1097-x

823 55. Mark R, Lyu X, Ng KR, Chen WN. Gene Source Screening as a Tool for Naringenin Production
824 in Engineered *Saccharomyces cerevisiae*. ACS Omega. 2019;4:12872–9.
825 https://doi.org/10.1021/acsomega.9b00364

826 56. Katahira R, Mittal A, McKinney K, Chen X, Tucker MP, Johnson DK, et al. Base-Catalyzed
827 Depolymerization of Biorefinery Lignins. ACS Sustainable Chem Eng. 2016;4:1474–86.
828 https://doi.org/10.1021/acssuschemeng.5b01451

829 57. Liu B, Falkenstein-Paul H, Schmidt W, Beerhues L. Benzophenone synthase and chalcone
830 synthase from *Hypericum androsaemum* cell cultures: cDNA cloning, functional expression,
831 and site-directed mutagenesis of two polyketide synthases. The Plant Journal. 2003;34:847–55.
832 https://doi.org/10.1046/j.1365-313X.2003.01771.x

833 58. Kim DH, Hwang HG, Jung GY. Optimum flux rerouting for efficient production of naringenin
834 from acetate in engineered *Escherichia coli*. Biotechnol Biofuels. 2022;15:90.
835 https://doi.org/10.1186/s13068-022-02188-w

836 59. Jones JA, Collins SM, Vernacchio VR, Lachance DM, Koffas MAG. Optimization of naringenin
837 and *p*-coumaric acid hydroxylation using the native *E. coli* hydroxylase complex, HpaBC.
838 Biotechnology Progress. 2016;32:21–5. https://doi.org/10.1002/btpr.2185

839 60. Parke D, Ornston LN. Toxicity Caused by Hydroxycinnamoyl-Coenzyme A Thioester
840 Accumulation in Mutants of *Acinetobacter* sp. Strain ADP1. Appl Environ Microbiol.
841 2004;70:2974–83. https://doi.org/10.1128/AEM.70.5.2974-2983.2004

842 61. Tong Y, Lyu Y, Xu S, Zhang L, Zhou J. Optimum chalcone synthase for flavonoid biosynthesis
843 in microorganisms. Critical Reviews in Biotechnology. 2021;41:1194–208.
844 https://doi.org/10.1080/07388551.2021.1922350

62. Christensen AB, Gregersen PL, Schroder J, Collinge DB. A chalcone synthase with an unusual substrate preference is expressed in barley leaves in response to UV light and pathogen attack.

63. Qiu Z, Han Y, Li J, Ren Y, Liu X, Li S, et al. Metabolic division engineering of *Escherichia coli* consortia for de novo biosynthesis of flavonoids and flavonoid glycosides. Metabolic Engineering. 2025;89:60–75. https://doi.org/10.1016/j.ymben.2025.02.001

64. Raytek LM, Saltzman BC, Sharma M, Lee SG, Dastmalchi M. Chalcone isomerase-like (CHIL) impedes the lactone shunt and modulates flux partitioning in isoflavonoid biosynthesis. Biochemical Engineering Journal. 2025;222:109853. https://doi.org/10.1016/j.bej.2025.109853

65. Waki T, Mameda R, Nakano T, Yamada S, Terashita M, Ito K, et al. A conserved strategy of chalcone isomerase-like protein to rectify promiscuous chalcone synthase specificity. Nat Commun. 2020;11:870. https://doi.org/10.1038/s41467-020-14558-9

66. Parke D, Ornston LN. Hydroxycinnamate (*hca*) Catabolic Genes from *Acinetobacter* sp. Strain ADP1 Are Repressed by HcaR and Are Induced by Hydroxycinnamoyl-Coenzyme A Thioesters. Appl Environ Microbiol. 2003;69:5398–409. https://doi.org/10.1128/AEM.69.9.5398-5409.2003

67. Biggs BW, Tyo KEJ. Aromatic natural products synthesis from aromatic lignin monomers using *Acinetobacter baylyi* ADP1 [Internet]. 2023 [cited 2024 Aug 18]. https://doi.org/10.1101/2023.08.24.554694

68. Cui H, Song MC, Lee JY, Yoon YJ. Microbial production of *O* -methylated flavanones from methylated phenylpropanoic acids in engineered *Escherichia coli*. Journal of Industrial Microbiology and Biotechnology. 2019;46:1707–13. https://doi.org/10.1007/s10295-019-02239-6

69. Zhu S-Y, Li N, Liu Z-H, Yuan Y-J, Li B-Z. Engineering budding yeast for the *de novo* synthesis of valuable flavanone derivatives. Green Chem. 2025;27:3477–93. https://doi.org/10.1039/D4GC05241B

Supplementary Files

This is a list of supplementary files associated with this preprint. Click to download.

- 260901SupplementaryMaterialsSantala.docx